

# Interaction Between Selected MoS<sub>2</sub> Nanoparticles and ZDDP Tribofilms

A. Tomala<sup>1</sup> · B. Vengudusamy<sup>1,5</sup> · M. Rodríguez Ripoll<sup>1</sup> · A. Naveira Suarez<sup>2</sup> · M. Remškar<sup>3</sup> · R. Rosentsveig<sup>4</sup>

Received: 27 March 2015 / Accepted: 23 May 2015 / Published online: 16 June 2015  
© Springer Science+Business Media New York 2015

**Abstract** Nanoparticles based on transition metal dichalcogenides (TMD) are considered to hold great promise as boundary lubricating additive/material for improving friction and wear of engineering functional surfaces. However, TMD nanoparticles cannot provide a comprehensive surface protection against oxidation, corrosion or sludge control. Therefore, the current lubricant developments may still have to depend on conventional additives such as zinc dialkyl dithiophosphate (ZDDP), and it is essential to understand the interaction of nanoparticles with such additives in order to explore how these nanoparticles could be commercially employed in fully formulated lubricants. This paper examines the tribological properties of three different nanoparticles: inorganic fullerene-like MoS<sub>2</sub>, rhenium-doped MoS<sub>2</sub> and MoS<sub>2</sub> nanotubes in steel and steel with preformed ZDDP tribofilm surfaces using a pin-on-disc-type tribometer under reciprocating sliding conditions. The resulting tribofilms have been evaluated using scanning electron microscopy coupled with energy-dispersive X-ray spectroscopy, transmission electron microscopy and atomic force microscopy. The results show that although the nanoparticles are able to reduce friction in all cases, the resulting tribofilm composition and morphology, and their lubricating mechanisms

are significantly different. The MoS<sub>2</sub> nanoparticles and nanotubes show good synergism with ZDDP, and tribofilms formed from nanoparticles exhibit improved friction and wear properties compared to that typically formed from ZDDP.

**Keywords** MoS<sub>2</sub> nanoparticles · MoS<sub>2</sub> nanotubes · ZDDP · Tribofilm · Friction · Wear

## 1 Introduction

The use of nanoparticles as boundary lubrication additives for lubricating oils has steadily gained attention during the last few years. Some typical nanoparticles have been reported to exhibit promising tribological properties, e.g. MoS<sub>2</sub>, nanotubes, WS<sub>2</sub>, include inorganic fullerene-(IF)-like nanoparticles made of metal dichalcogenides (IF-MoS<sub>2</sub>), rhenium-doped MoS<sub>2</sub> (Re/IF-MoS<sub>2</sub>). In particular, IF-MoS<sub>2</sub> nanoparticles appear to be the most widely explored ones [1], probably due to their wide range of promising applications (e.g. improving mechanical properties of nanocomposites [2], solid lubricants [3]) and non-hazardous to the environment [4]. In general, IF-like nanoparticles (IF-NPs) comprise a diverse types of nanomaterials having in common closed-cage structures made of layered (2D) and non-layered (3D) compounds [5]. Technological advancements in the past decade have made possible the manufacturing of nanoparticles in several different geometries such as nanotubes, fullerenes and onions.

Although several different types of IF-NPs are commercially available in the market, the knowledge on their lubricating properties/mechanisms is limited. One of the

✉ A. Tomala  
tomala@ac2t.at

<sup>1</sup> AC2T research GmbH, Wiener Neustadt, Austria  
<sup>2</sup> Luleå University of Technology, Luleå, Sweden  
<sup>3</sup> Institut “Jožef Stefan”, Ljubljana, Slovenia  
<sup>4</sup> Weizmann Institute of Science, Rehovot, Israel  
<sup>5</sup> Present Address: Klüber Lubrication München SE & Co. KG, Munich, Germany

commonly postulated mechanisms with these nanoparticles comprise three steps, namely (1) rolling of nanoparticles, acting like a nano- or microball bearing (Fig. 1a), (2) deformation of nanoparticles leading to surface enhancement/healing, e.g. filling in cracks, preventing asperity contact. (Fig. 1b) and (3) exfoliation and deposition of nanoparticles on to surfaces (Fig. 1c).

However, it appears that the above-mentioned mechanisms were derived based on experiments with model fluids [6–16] or on tests under dry contact conditions, mostly on steel surfaces. Some recent studies have explored the potentials of nanoparticles with non-ferrous surfaces such as diamond-like carbon (DLC) coatings [10, 11]. However, the results reported with DLCs appear to be contradictory as nanoparticles were claimed to be ineffective on DLC [10], while another work reported the opposite [11]. These results hint that benefits of nanoparticles could be significantly influenced by contact materials, nanoparticle structure, surface roughness of test specimens, test conditions, etc. [12]. Examples of how nanoparticle size, structure or structural defect could affect their tribological properties have been explored by Rabaso et al. [13]. These studies reported that nanoparticles with structural defects, i.e. poorly crystalline IF-MoS<sub>2</sub>, show earlier friction reduction compared to those without structural defects. It is believed that poor crystallinity promotes easy and quick exfoliation of nanoparticles. Furthermore, MoS<sub>2</sub> nanotubes (MoS<sub>2</sub>-NT) were reported to be more or much more effective with rough steel surfaces compared to smooth ones [14].

On the existing literature, the behaviour of nanoparticles under dry condition or as a mixture in base oil solution has been extensively investigated. However, when intended to use as fully formulated lubricants in a real application, many factors could influence the performance of MoS<sub>2</sub> nanoparticles, which have not been systematically addressed so far. Very little work exists on the interactions of nanoparticles with conventional additives. A very recent article of Rabaso et al. [15] has investigated IF-MoS<sub>2</sub> nanoparticles functionality in fully formulated lubricants, claiming that there is no effect of nanoparticles on the behaviour of the oil, due to excess of dispersants used in commercial oil, which prevent the agglomeration of particles. Another work of Aldana et al. [16] has explored

great potential of WS<sub>2</sub> nanoparticles when mixed with conventional anti-wear additive such as zinc dialkyl dithiophosphate (ZDDP) and reported that nanoparticles were able to form nanosheets and strongly reduce friction.

Whether or not the functionality of such nanoparticles will be compromised, when used along with other surface active additives (that are typically used in fully formulated lubricants), remains largely unknown. It is therefore important to understand these interactions in order to be able to design efficient nanoparticle-based fully formulated lubricants. To shed some light in this direction, this article has attempted to study the compatibility/interactions between three different nanoparticles [inorganic fullerene-like MoS<sub>2</sub> (IF-MoS<sub>2</sub>), rhenium-doped MoS<sub>2</sub> (Re/IF-MoS<sub>2</sub>) and MoS<sub>2</sub>-NT] and ZDDP, to understand how their lubricating properties differ both when used alone (in base oil) and together with ZDDP. In addition, while most of the previous works focused on high contact pressures in the order of 1 GPa, this study has used a relatively much lower contact pressure (141 MPa) to see whether and how such nanoparticles could be used in automotive engine applications.

## 2 Materials and Experimental Details

### 2.1 Materials

#### 2.1.1 Test Specimens

The test specimens used were AISI 52100 steel pins and discs of hardness 815 HV1 and 760 HV1, and roughness  $R_a$  0.13 and 0.05  $\mu\text{m}$ , respectively. The specimens were cleaned before the tests in ultrasonic bath first with toluene (10 min) and then with petroleum ether (10 min).

#### 2.1.2 Lubricants and Nanoparticles

The lubricants used in this study were (a) additive-free poly- $\alpha$ -olefin (PAO) base oil, (b) PAO with ZDDP and (c) PAO with nanoparticles. The base fluid used in this study was PAO 4 having viscosity of 24.6 mm<sup>2</sup>/s at 40 °C and 4 mm<sup>2</sup>/s at 100 °C. The ZDDP used had a primary alkyl structure with 99 % purity and was used at 2 wt% concentration in both base oil and base oil with NPs. The ZDDP lubricant solutions were prepared using an ultrasonic bath to dissolve ZDDP in the base oil, and the temperature was maintained below 40 °C during the dissolving procedure. The nanoparticles (NPs) investigated in this study were inorganic fullerene-like MoS<sub>2</sub> (which hereafter will be referred to as IF-MoS<sub>2</sub>), rhenium-doped MoS<sub>2</sub> (which hereafter will be referred to as Re/IF-MoS<sub>2</sub>) and MoS<sub>2</sub>-nanotubes with a mixture of co-axial

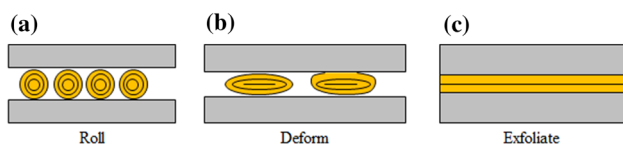


**Fig. 1** Illustration of lubrication mechanisms with MoS<sub>2</sub>-based nanoparticles and nanotubes

nanotubes and “mama”-tubes with MoS<sub>2</sub> nanoonions in it (which hereafter will be referred to as MoS<sub>2</sub>-NT), and were used at 5 wt % concentration. The suspension of oil and NPs was thoroughly mixed using ultrasound (500 W, 50 Hz) for 1 h just before being used in experiments. There are several references [11, 13] pointing out a possible effect of ultrasonic treatment on nanoparticle damage. As a consequence, treated nanoparticles can be more easily exfoliated under shear stress.

The two IF-NPs, namely IF-MoS<sub>2</sub> and Re/IF-MoS<sub>2</sub>, were supplied by the Department of Material and Interfaces, Weizmann Institute of Science, Israel. The IF-NPs were synthesised by quartz reactor using MO<sub>3</sub> powder as precursor and H<sub>2</sub>S/H<sub>2</sub> gas at a temperature of 800–830 °C, and a final annealing step at 870 °C, according to the procedure published in Ref. [8, 9, 12]. For the synthesis of Re/IF-MoS<sub>2</sub>, the fundamental reaction parameters were slightly modified from those employed in Ref. [8], and the Re<sub>x</sub>Mo<sub>1-x</sub>O<sub>3</sub> ( $x < 0.01$ ) precursor powder was prepared in a specially designed auxiliary reactor [9, 12]. The concentration of Re in the Re/IF-MoS<sub>2</sub> is about 100 ppm (0.01 at.%). A detailed description about the synthesis can be found elsewhere [9]. The size of the IF-MoS<sub>2</sub> is approximately 120–130 nm (mean value) in diameter. Moreover, some 50 nm but also 250 nm nanoparticles can be found. Figure 2a, b shows accordingly a SEM and TEM images of

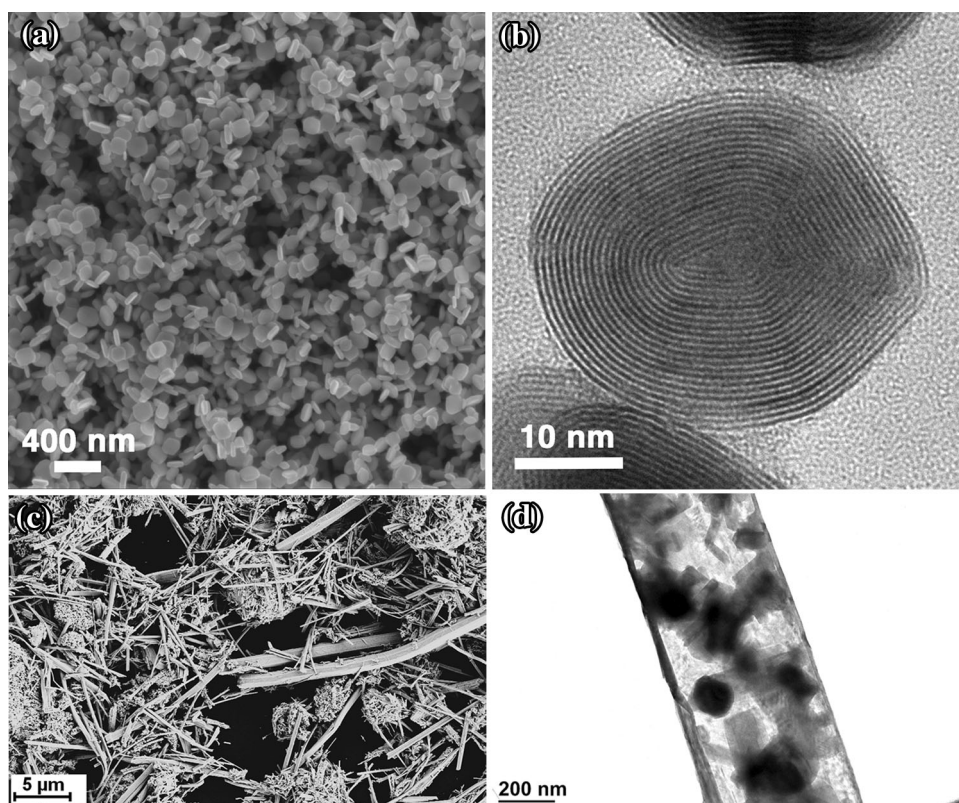
the Re/IF-MoS<sub>2</sub> nanoparticles. There is no visual difference between Re-doped and undoped IF-MoS<sub>2</sub>; this is the reason why only one type is shown here.

The MoS<sub>2</sub>-NT were supplied by the Solid State Physics Department, Jožef Stefan Institute, Ljubljana, Slovenia. The MoS<sub>2</sub>-NT are partially filled with MoS<sub>2</sub> nanoonions, and because of this cage structure, they are often called “mama”-tubes. They are approximately 100 nm up to 500 nm in diameter and up to 20 μm long; the walls of the tubes are <10 nm thick. The MoS<sub>2</sub>-NT were synthesised by the procedure reported in [11], which is by the sulphurisation of Mo<sub>6</sub>S<sub>4</sub>I<sub>6</sub> nanowires at 810 °C in a reactive gas composed of 98 vol% Ar, 1 vol% of H<sub>2</sub>S and 1 vol% of H<sub>2</sub> for 1 h. The pristine MoS<sub>2</sub>-NT kept the original, hedgehog self-assembly [14] of the starting material, which can be easily dispersed in polar media using ultrasound. Figure 2c, d shows accordingly a SEM and TEM images of a mixture of co-axial nanotubes and “mama”-tubes with MoS<sub>2</sub> nanoonions inside MoS<sub>2</sub>-NT.

## 2.2 Tribological Test Set Up

The pin-on-disc tests were performed using a SRV<sup>®</sup> tribometer (Optimol, Munich), where a 3-mm-diameter steel pin was loaded and reciprocated against a stationary steel disc lubricated by a lubricant solution under boundary

**Fig. 2** SEM (a) and TEM (b) images of Re/IF-MoS<sub>2</sub> nanoparticles. SEM (c) and TEM (d) images of mixture of co-axial nanotubes and “mama”-tubes with MoS<sub>2</sub> nanoonions inside MoS<sub>2</sub> nanotubes



lubricated, pure sliding condition. The oscillation frequency was 8 Hz and the stroke 3 mm, which gives an average sliding speed of 0.048 m/s. The pins had a diameter of 3 mm, and their contact surface was polished/ground to a flat end. The normal load was set to 1000 N, which corresponded to a mean initial contact pressure of 141 MPa. This simulates a contact condition similar to that observed in automotive engines (e.g. cam/tappet and ring/liner). All tests were conducted at 40 °C.

Tests were performed in three experimental series, as listed in Table 1. In series I, tests with PAO, PAO + ZDDP and PAO + nanoparticles were conducted for 2 h, which resulted in a total sliding distance of 345.6 m. In series II, nanoparticle tests were conducted on ZDDP tribofilm-containing surfaces. This was done by testing first in PAO + ZDDP solution for 2 h, followed by testing in PAO + nanoparticles for 2 h, covering a total sliding distance of 691.2 m.

## 2.3 Surface Analyses

After tribological tests, the tested specimens were rinsed in petroleum ether before the wear tracks were examined by using a series of surface characterisation instruments including optical interferometer, SEM/EDX, AFM and TEM.

### 2.3.1 Surface Topography

Surface topography of the tested samples was evaluated using a Leica DCM 3D—combining interferometric and confocal microscopy (Leica, Japan). Surface roughness was measured before and after the tests according to ISO 4287. The Leica Map Premium 0.2.0190 software was used for wear volume analysis. Volume analysis method estimates the volume between the worn surface and a reference plane. The reference plane was set as the average height of the unworn area outside the wear track. The wear volume was calculated for the whole wear track, and only the area under the reference plane was considered. Then, wear coefficients ( $K$ ) of pin and disc specimens were calculated using the Archard's equation:

$$K = \frac{V}{F \times S}$$

**Table 1** Test matrix employed in this study. Values shown in the bracket indicate the test duration

Series I	Series II (tests on preformed ZDDP tribofilm with NPs)
PAO (2 h)	–
PAO + ZDDP (2 h)	PAO + ZDDP (4 h)
PAO + MoS <sub>2</sub> -NT (2 h)	PAO + ZDDP (2 h) and PAO + MoS <sub>2</sub> -NT (2 h)
PAO + IF-MoS <sub>2</sub> (2 h)	PAO + ZDDP (2 h) and PAO + IF-MoS <sub>2</sub> (2 h)
PAO + Re/IF-MoS <sub>2</sub> (2 h)	PAO + ZDDP (2 h) and PAO + Re/IF-MoS <sub>2</sub> (2 h)

where  $V$  is the wear volume (m<sup>3</sup>),  $F$  is the normal load (N), and  $S$  is the sliding distance (m).

In addition, wear tracks on the pins and discs were visually inspected using an optical microscope.

### 2.3.2 SEM/EDX

The SEM micrographs were obtained using a FEI Quanta 200 ESEM FEG. It is equipped with a Schottky field emission gun (FEG) for optimal spatial resolution. The instrument can be used in high-vacuum mode (HV), low-vacuum mode (LV) and the so-called environmental SEM (ESEM) mode. This makes it possible to study samples in pressures up to 5 Torr. The microscope is equipped with an Oxford Inca Energy-Dispersive X-ray (EDX) system for chemical analysis. The spectra were collected at 20 keV, and the acquisition time was 60 s.

### 2.3.3 AFM

Measurements were taken with an AFM MFP-3D atomic force microscope (by Asylum Research, Santa Barbara, CA) in contact, constant force mode using non-conductive silicon nitride cantilevers with a spring constant  $k = 1$  N/m and a resonant frequency  $f_0 = 38$  kHz (Veeco). The main measurement parameters were: a scan size from  $10 \times 10$  to  $70 \times 70 \mu\text{m}^2$  (512 scan points and 512 scan lines), a scan rate of 1 Hz, scan angle of 90° and a set point at 20 nN in contact mode. The recorded data were both trace/retrace of height, deflection and lateral force. Scanning was performed across the sliding direction and in the axis perpendicular to the long axis of the cantilever, and at the centre and the edge of the wear scars.

Also, force–displacement curves were obtained at fixed positions on the specimens inside (blue curves) and outside (red curves) the wear tracks. These are presented as deflection of the cantilever (nm) versus LVDT ( $\mu\text{m}$ ) (linear variable differential transformer is a position sensor measuring linear displacement).

Hysteresis during contact indicates that some plastic deformation has occurred while load was applied to the surface, due to the presence of a relatively soft surface film formed either by nanoparticles, ZDDP and/or both.

### 2.3.4 TEM

TEM measurements were taken on a TECNAI F20 field emission TEM operating at 200 kV. For EDX analysis, we used an Apollo XLTW SDD detector from AMETEK (windowless detector). Images were recorded with a Gatan Orius CCD camera STEM images were recorded using a high-angle annular dark field detector.

## 3 Results

Friction and wear properties of the selected nanoparticles were evaluated using pin-on-disc tests. PAO4 base oil was mixed 5 % weight MoS<sub>2</sub>-NT, nanoparticles, and Re-doped nanoparticles. A test using only base oil was performed to be used as reference. Each test was repeated at least twice for statistical reasons, and variation was always <10 %.

### 3.1 Friction and Wear

The evolution of friction as a function of time and sliding distance for base oil, base oil with ZDDP and base oil with nanoparticles on fresh steel surfaces (series I tests) is shown in Fig. 3. The results show that higher friction (ca. 0.13) is achieved when using base oil without nanoparticles (i.e. PAO and PAO + ZDDP). ZDDP shows higher friction coefficient similar to that of base oil. This is reasonable taking into account that ZDDP forms rough tribofilms, which has been widely reported [17]. While IF-MoS<sub>2</sub> shows slightly lower friction (ca. 0.09), both MoS<sub>2</sub> NT (ca. 0.06) and Re/IF-MoS<sub>2</sub> (ca. 0.04) show significantly lower friction than PAO and ZDDP. With MoS<sub>2</sub>-NT, friction was initially higher (0.1), which then reduced after running-in, reaching 0.05 at the end of 2 h. In

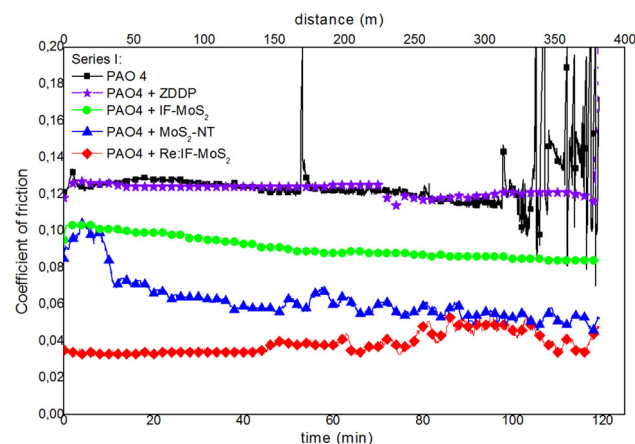


**Fig. 3** Evolution of friction for PAO, ZDDP and nanoparticles with fresh steel surfaces (series I tests)

contrast to IF-MoS<sub>2</sub>, Re/IF-MoS<sub>2</sub> shows low friction from the start of the test (0.04), indicating the significance of Re doping to IF-MoS<sub>2</sub>. It should also be noted that Re/IF-MoS<sub>2</sub> achieves steady-state conditions faster compared to the other two nanoparticles.

The evolution of friction for nanoparticles with ZDDP tribofilm-containing surfaces (i.e. series II tests) is shown in Fig. 4. As can be seen in Fig. 4, friction in the initial 2 h was higher (0.13), resulting solely from ZDDP (verified and shown later in Fig. 11b with EDX analysis which showed the presence of Zn and P on the wear track). When changed to nanoparticle solution after 2 h of initial rubbing in ZDDP, all three nanoparticles showed immediate reduction in friction to a value of about 0.05. This indicates the effective presence of nanoparticles at the contact interface. It appears that nanoparticles get easily embedded on to the preformed, soft ZDDP tribofilm; thus, contact is predominantly nanoparticle-on-nanoparticle instead of ZDDP tribofilm-on-ZDDP tribofilm. These results can be

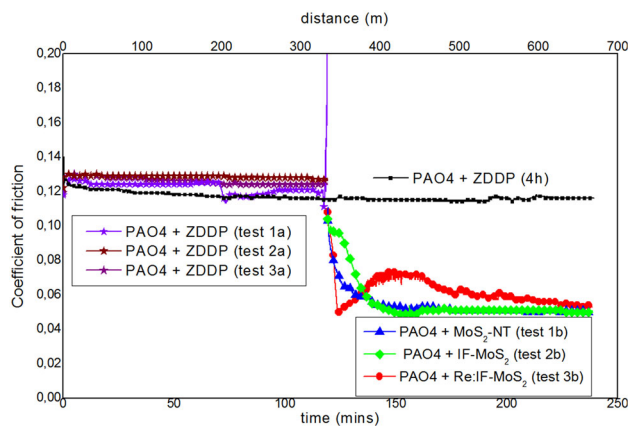


**Fig. 4** Evolution of friction for nanoparticles with ZDDP tribofilm-containing surfaces (series II tests)

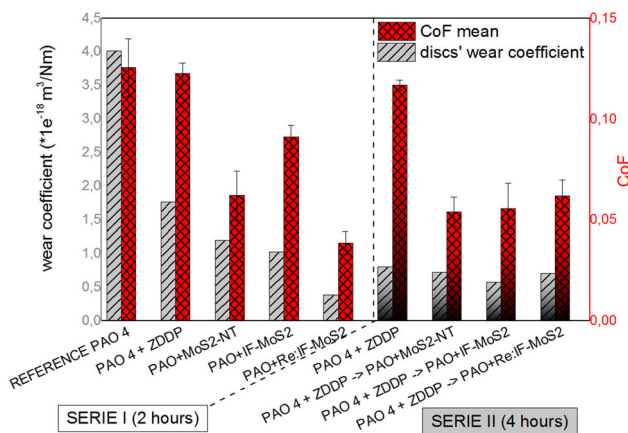


**Fig. 5** Friction and wear coefficients from series I (fresh steel surfaces) and II (ZDDP tribofilm-containing surfaces) tests

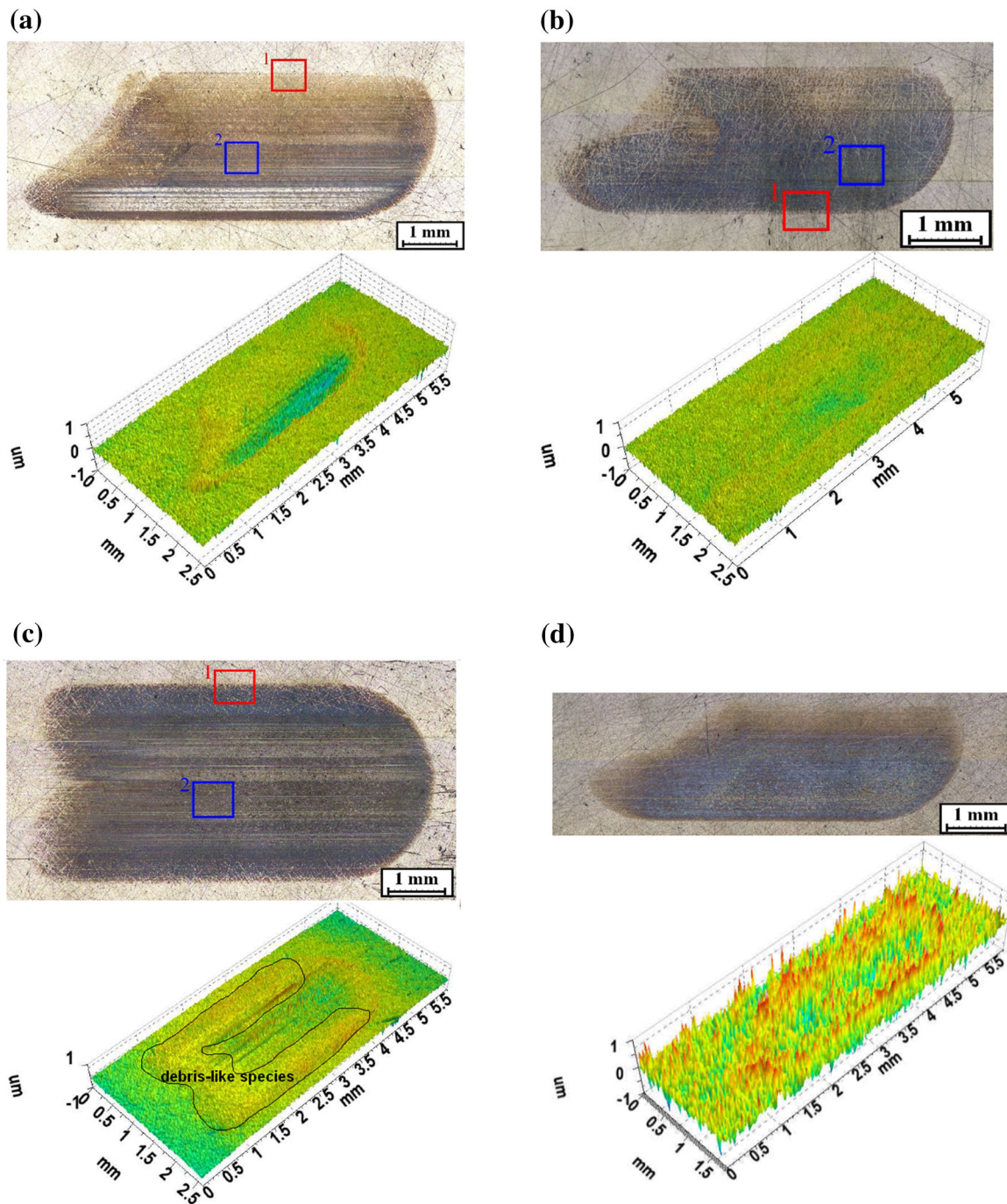


**Fig. 6** Optical microscope images of disc surfaces after rubbing in **a**, **f** NT, **b**, **g** IF-MoS<sub>2</sub>, **c**, **h** Re/IF-MoS<sub>2</sub>, **d**, **i** PAO + ZDDP (series I-2 h test and series II-4 h test) and **e** PAO4 (series I, 2 h test) **a–e** series I

tests and **f–i** series II tests. *Rectangular* areas 1 and 2 indicate the locations for AFM measurements (Figs. 7, 9)

directly compared to those obtained in the literature concerning the interactions between WS<sub>2</sub> and ZDDP additives [16]

The wear coefficients of disc along with the friction coefficients obtained in series I and series II tests are shown in Fig. 5. Disc wear is used to characterise the wear

performance of nanoparticles, since pin wear was negligible for all nanoparticles investigated in this study.

With steel surfaces (series I tests), the disc wear with additive-free PAO was the highest, which, however, reduced when AW (anti-wear) additive ZDDP was used. This is not surprising as ZDDP forms thick tribofilms that prevent

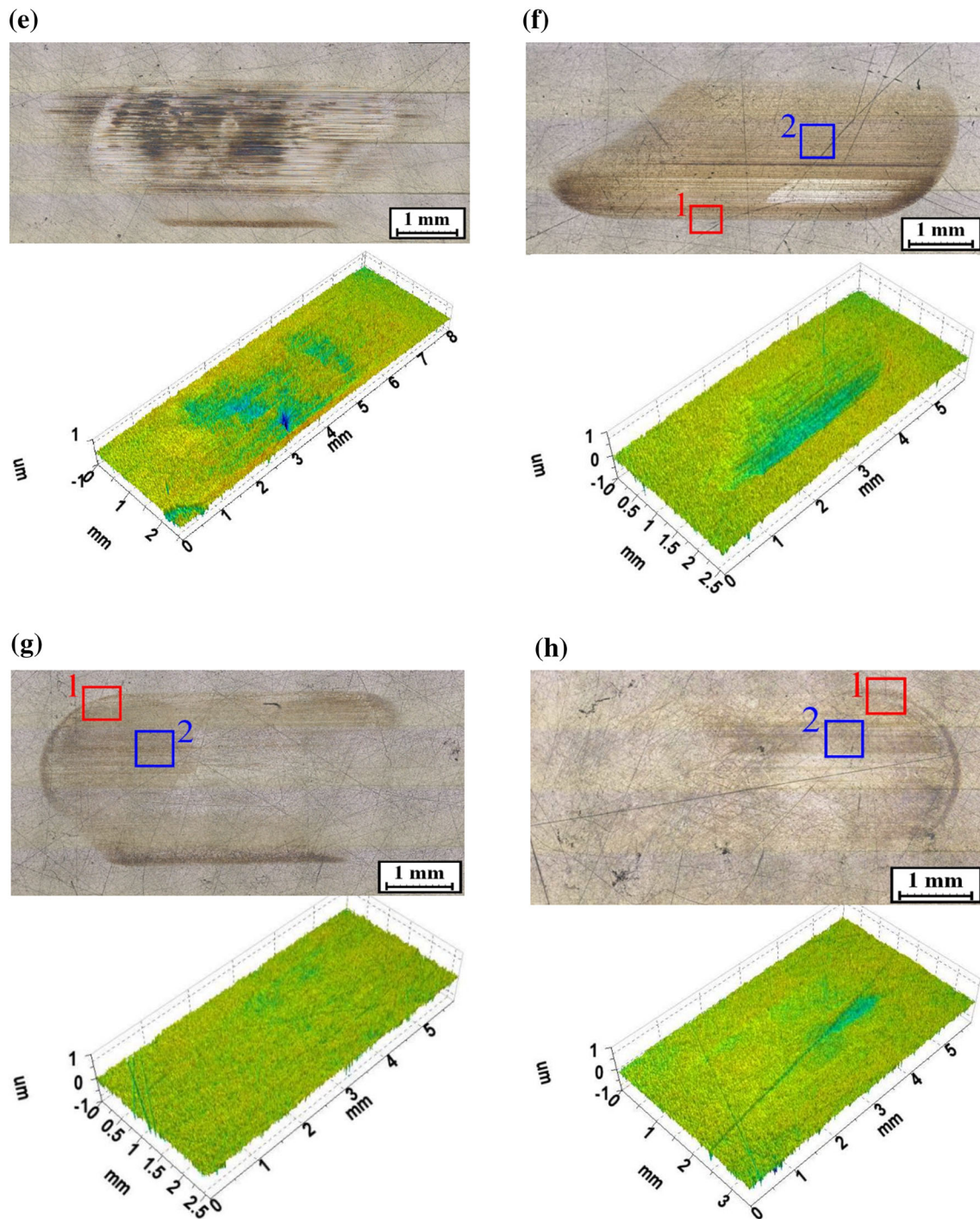


**Fig. 6** continued

surfaces from wearing. It is interesting to note that all three nanoparticles investigated in this study showed lower disc wear than PAO with ZDDP. In particular, Re/IF-MoS<sub>2</sub> showed in Fig. 5 significantly lower wear ( $0.4 \times 10^{-18} \text{ m}^3/\text{Nm}$ ). The wear values reported here for nanoparticles are lower than those typically reported for DLC coatings with ZDDP [18]. These results suggest that nanoparticles can be

considered as potential candidates for applications with focus on lower friction and wear, and more important even in the absence of widely used anti-wear additives, such as ZDDP. With preformed ZDDP tribofilm-containing surfaces (series II tests), disc wear with PAO and ZDDP and PAO with nanoparticles remain similar (Fig. 5). This indicates that changing to nanoparticles after 2-h rubbing in ZDDP

(i)

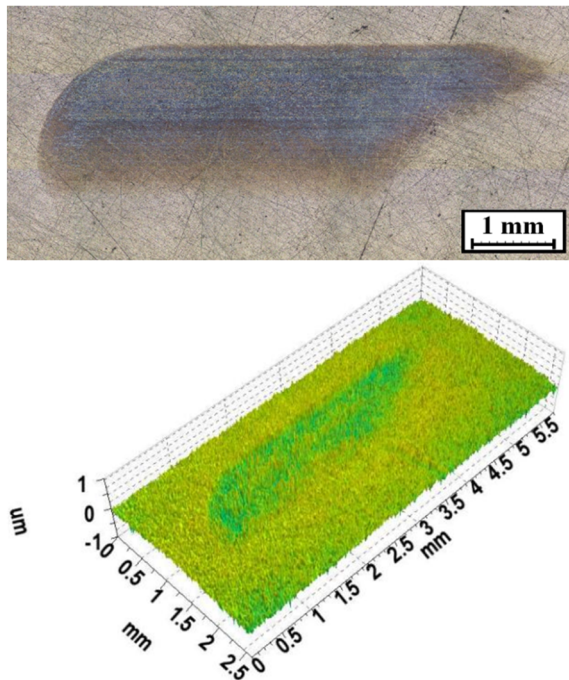


Fig. 6 continued

does not degrade the original anti-wear properties of the preformed ZDDP tribofilm. This, further, suggests that nanoparticles were either rolling or got deposited on top of the ZDDP tribofilm, allowing the contact to operate with low friction without compromising the wear performance. The wear tracks on discs from series I and II tests are shown in Fig. 6a–e, f–i, respectively. As can be seen in Fig. 6e, base oil showed large wear scar, wear depth and material loss. A deep wear scar is visible with a width similar to the pin diameter and scratches produced by abrasion. While PAO + NP showed smooth wear scar with less wear depth on disc (Fig. 6b), disc wear depth obtained with Re/IF-MoS<sub>2</sub> was also less, but wear scar was surrounded by debris-like species (Fig. 6c).

Optical microscopy images for series II tests (Fig. 6f–h) except test with PAO + ZDDP (Fig. 6i) show brighter wear tracks compared to wear tracks obtained in series I. This can be attributed either to the temperature—lower frictional heat generated in series II—or to different action mechanism of nanoparticles in the tribocontact. Confocal microscopy observations for series II tests showed that PAO + ZDDP tests followed by testing in PAO + particles (Fig. 6f–h) result in smooth wear scar compared to the tests with PAO + ZDDP (Fig. 6i). Negligible wear depth on disc was observed for PAO + ZDDP tests followed by testing in PAO + IF-MoS<sub>2</sub> (Fig. 6g). These results confirm that nanoparticles boost the anti-wear performance of widely used additives such as ZDDP.

### 3.2 Tribofilm Formation

The formation of tribofilms when using nanoparticles is assessed by comparing surface morphology using SEM and AFM shown in Figs. 7 and 8, respectively, and by comparing chemical composition of surface layers using EDX, shown in Tables 2 and 3 for series I and II tests, respectively. The SEM micrographs, AFM images and EDX measurements were taken on a representative area (rectangular marks numbered as 2 on Fig. 6) that reflects the surface conditions well. It should be noted that a model test was conducted to ensure that ZDDP tribofilm formed (verified by EDX, results shown later in Fig. 12b) in the first 2 h of series II tests, i.e. prior to changing from ZDDP to nanoparticle solution.

AFM topography measurements are presented for series I (Fig. 8a–c) and II (Fig. 8d–f). Wear tracks obtained after testing PAO + nanoparticles (series I, Fig. 8a–c) show smoother surfaces compared to those pretested with ZDDP (series II, Fig. 8d–f). In all cases, surface enhancement effect of nanoparticles can be observed due to the high amount of particles filling the pits and cracks on the tribofilm surface.

Both with steel (series I tests) and ZDDP-containing tribofilm (series II tests) surfaces, formation of nanoparticle-derived tribofilms is evident from EDX measurements (Tables 2, 3), indicated by the presence of Mo and S elements on the wear track (although not with Re/NP in series II tests, the reason for this is discussed later). It can be seen from SEM micrographs that both with series I and II tests, nanoparticles form pad-like structures. This is indicated by dashed lines in micrographs from series I tests, shown in Fig. 7a–c. Such pad-like features are also illustrated clearly in Fig. 9a, b, which shows magnified micrographs obtained from wear tracks of NP tribofilm formed on steel surface and NP tribofilm formed on steel surface with preformed ZDDP tribofilm. These pads, indicated by dashed lines in Fig. 9a, contain 1.0 at.% Mo and 1.5 at.% S, indicating that these are MoS<sub>2</sub>-derived tribofilms. It should be noted from Fig. 9b that tribosurface formed from NP-lubricated steel containing preformed ZDDP tribofilm shows more pits. But, these are not pits instead thick non-homogenous pads, showing border of large pads as pits.

Formation of similar pad-like structures is widely reported when using anti-wear additive ZDDP on steel surfaces [19]. An example of this, adapted from one of the authors' earlier work (Vengudusamy et al. [20]), is shown in Fig. 9c [20]. Although NP formed pad-like structures both with steel and steel with preformed ZDDP tribofilm, they were not as distinctive as those formed solely from ZDDP (Fig. 9c). The pads shown in Fig. 9b look similar to those formed solely from ZDDP (Fig. 9c) as the surface had pretreated ZDDP films. However, the pads shown in

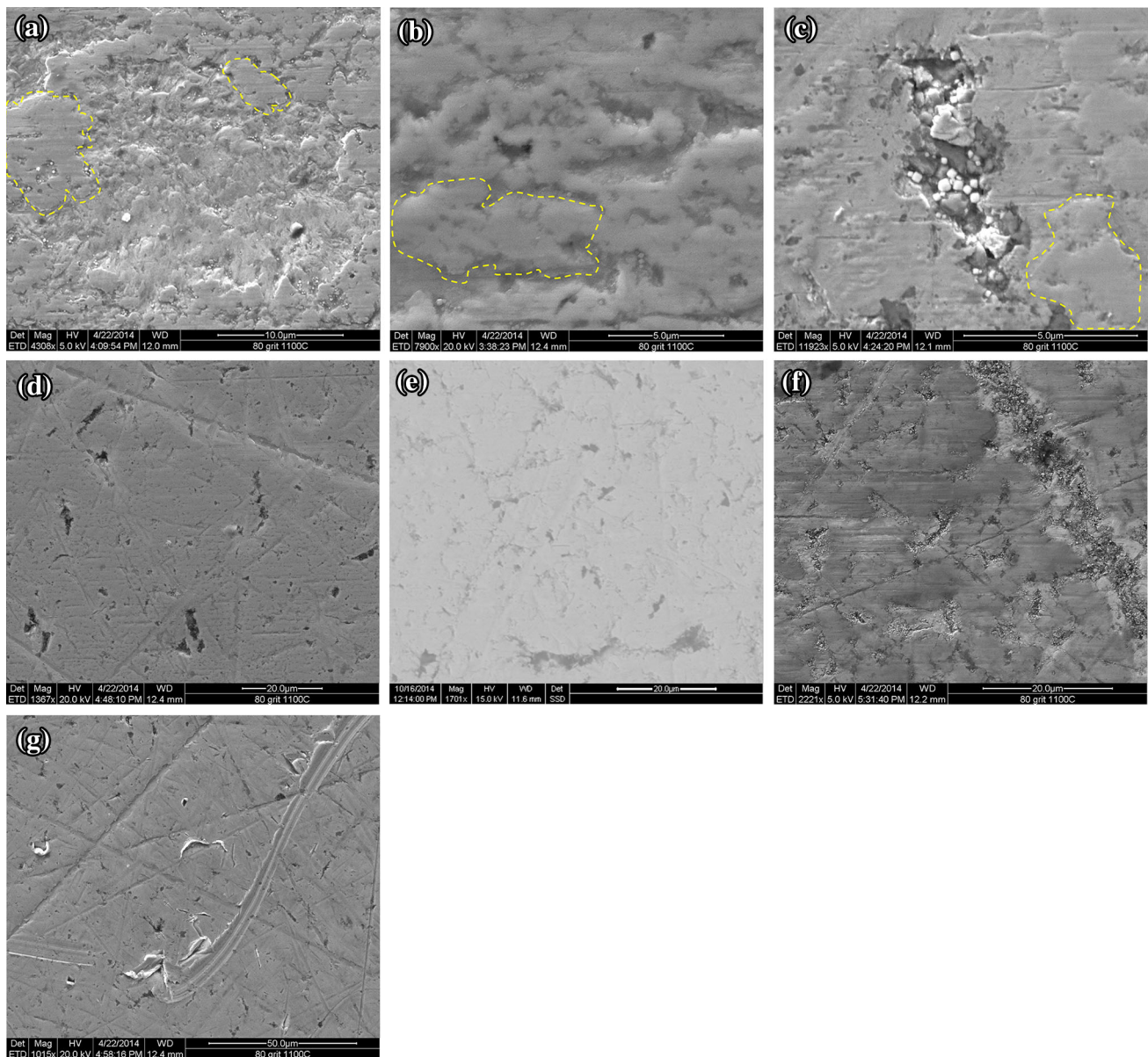


**Fig. 7** SEM micrographs of disc surfaces after rubbing in **a, d** MoS<sub>2</sub>-NT, **b, e** IF-MoS<sub>2</sub>, **c, f** Re/IF-MoS<sub>2</sub>. A reference fresh steel surface

micrograph is shown in **g**. **a–c** indicate series I tests, and **d–f** indicate series II tests. *Dashed lines* in **a–c** indicate pad-like film structure

Fig. 9b appear to have flattened by rolling over of NP, which presumably resulted in the formation of pit-like borders for the pads. Also, surfaces from Re/IF-MoS<sub>2</sub> showed similar pits on wear track (Fig. 7c), and these are also believed to be formation of large pads with borders appearing as pits, similar to those observed with IF-MoS<sub>2</sub>.

AFM topography scans are shown in Fig. 10. The measurements were taken at the border of the wear track, i.e. an area that covers both wear track and untested surface (indicated as rectangular mark numbered 1 on Fig. 6a–h). These results, as seen in Fig. 10, reveal that in case of test series II with nanoparticles (prerubbing with ZDDP), the

surface is smoother inside the wear tracks compared to outside. Typically, contacts lubricated with additive-free PAO produce rougher wear tracks (results not shown). These results suggest that contacts lubricated with nanoparticles caused smooth running-in. Also, in all cases, original polishing marks (showing microgrooves) of steel surface are seen, indicating that tribofilms were formed on the surface and covered the microgrooves. Furthermore, it should be noted from Fig. 10 that AFM scans obtained at the border region between outside/inside wear tracks show no striking height differences for all nanoparticles used in this study. This can be attributed to high surface roughness

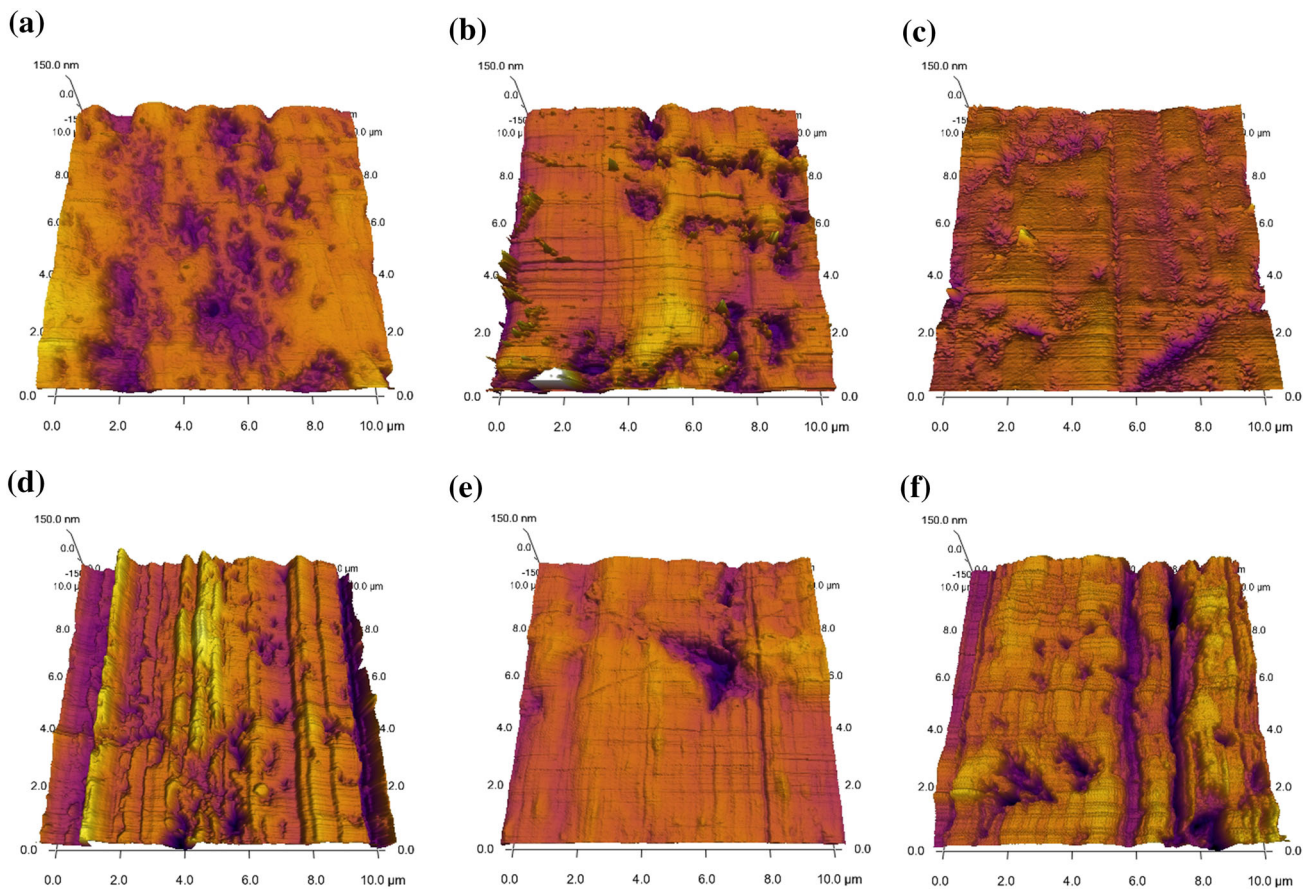


**Fig. 8** AFM images from wear tracks formed on disc surfaces after rubbing in **a, d** MoS<sub>2</sub>-NT, **b, e** IF-MoS<sub>2</sub> and **c, f** Re/IF-MoS<sub>2</sub>. **a–c** indicate series I tests, and **d–f** indicate series II tests

**Table 2** EDX measurements on steel surfaces tested in NT, IF-MoS<sub>2</sub> and Re/IF-MoS<sub>2</sub> (series I tests)

Element	MoS <sub>2</sub> -NT	IF-MoS <sub>2</sub>	Re/IF-MoS <sub>2</sub>
<i>Atomic concentration (%)</i>			
C K	52.2	48.6	61.8
O K	6.5	6.1	2.4
Si K	–	0.3	13.8
S K	6.0	1.4	10.5
Cr K	–	0.6	–
Fe K	31.8	42.0	5.2
Mo K	3.5	1.0	6.3

**Table 3** EDX measurements on ZDDP tribofilm-containing disc surfaces tested in NT, IF-MoS<sub>2</sub> and Re/IF-MoS<sub>2</sub> (series II tests)

Element	MoS <sub>2</sub> -NT	IF-MoS <sub>2</sub>	Re/IF-MoS <sub>2</sub>
<i>Atomic concentration (%)</i>			
C K	26.8	23.4	36.0
O K	7.0	8.0	12.0
Si K	1.4	2.0	0.5
P K	–	0.5	1.1
S K	0.3	0.5	–
Cr K	1.1	1.1	1.5
Fe K	63.0	63.7	47.9
Zn K	–	0.8	0.5
Mo K	0.4	–	0.5

outside the scar, so that any tribofilm formation is not measurable by AFM height scans. However, tribofilm formation using NPs was already verified by EDX measurements (Table 2).

In order to analyse in detail the tribofilms formed from NP on steel (series I) and ZDDP tribofilm-containing steel (series II), surfaces were further analysed on TEM by making a

transversal cut using FIB, as shown in Figs. 11 and 12. The cross section of the tribofilm formed from NP on bare steel surface is shown in Fig. 11a. The chemical mapping (Fig. 11b) and EDS measurements (Fig. 11c) taken on the tribofilm area confirm the presence of Mo. These results indicate that bulk portion of the tribofilm consists of oxides

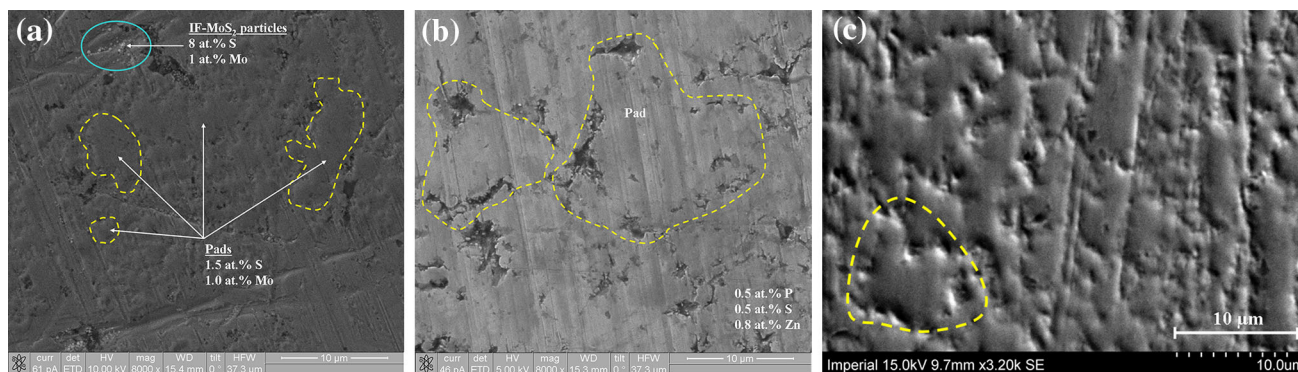


**Fig. 9** SEM micrographs of **a** NP tribofilm formed on steel surface and **b** NP tribofilm formed on steel surface with preformed ZDDP tribofilm and **c** typical ZDDP tribofilm formed on steel surface (adapted from [20]). Dashed polylines indicate pads, and solid ellipse in **b** indicates the presence of IF-MoS<sub>2</sub> nanoparticles

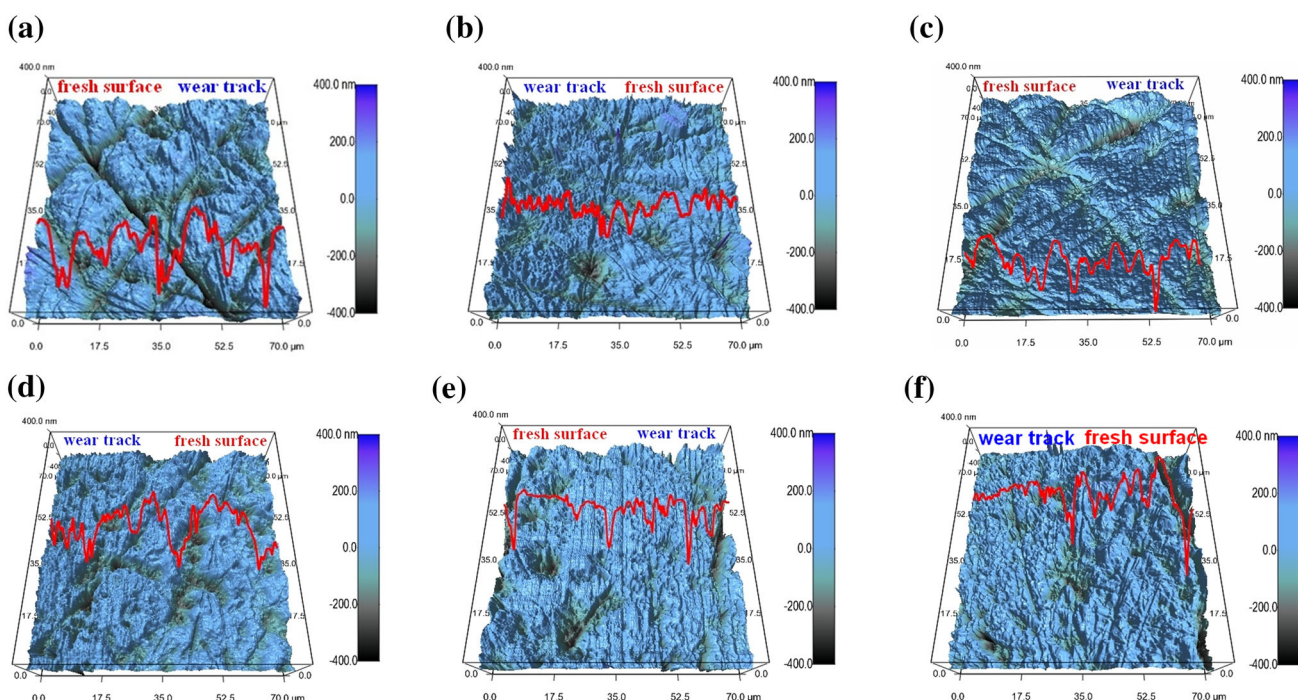


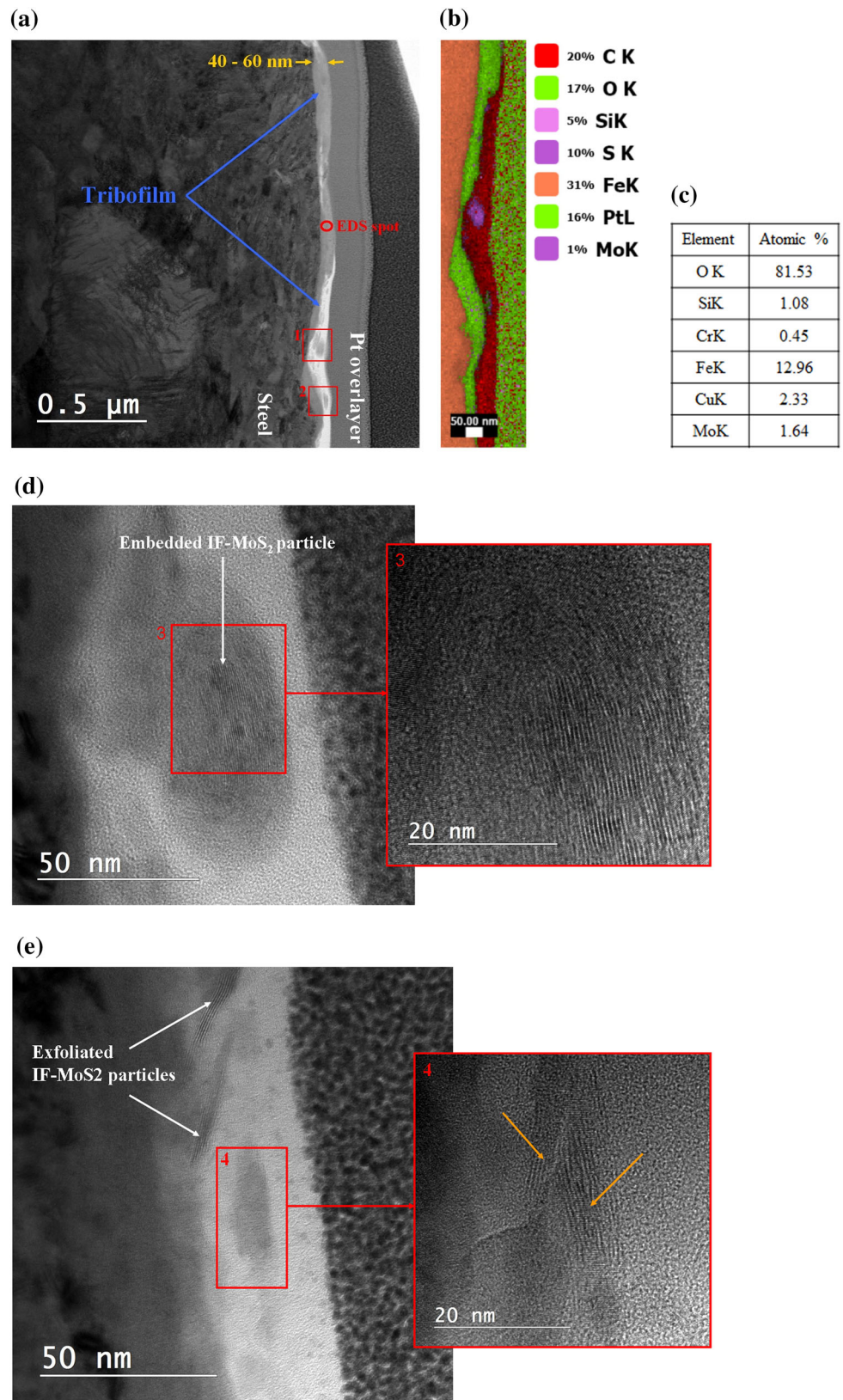
**Fig. 10** AFM images obtained in the border between inside and outside the wear track after rubbing in **a, d** MoS<sub>2</sub>-NT, **b, e** IF-MoS<sub>2</sub> and **c, f** Re/IF-MoS<sub>2</sub>. **a–c** series I tests and **d–f** series II tests

(Fig. 11b). Similar oxide formation has been reported earlier by Tannous et al. [10]. MoS<sub>2</sub>-derived products are found predominantly to be trapped (Fig. 11b, d) and/or exfoliated (Fig. 11e) within the bulk layer of the tribofilm. This can be explained as gradual exfoliation and a transfer of molecular sheets onto the asperities of the reciprocating surfaces, and it is in agreement with the lubrication mechanism of the IF-MoS<sub>2</sub> proposed in the literature [6, 10]. This should explain the reason for the presence of small amounts of sulphur or molybdenum in the iron oxide layer (Fig. 11b). The layer was also found to have some small amounts of silicon at the top surface, and this is attributed to silicon powder suspension used

in the final polishing stage of the discs. Although the thickness of the tribofilm varied between 40 and 60 nm, the inner IF-MoS<sub>2</sub> lamellar structures sheets, which are present in the tribofilm, are only about 10–15 nm (as shown of Fig. 11d, e).

The cross section of NP tribofilm formed on steel surface containing preformed ZDDP film is illustrated in Fig. 12a. It shows pale, light-coloured bubble-like structures within the tribofilm, which were not seen previously on the film formed on steel surface (Fig. 11a). Detailed and focused TEM analysis has shown that these structures are perfectly amorphous and are in fact artefacts resulting from sensitivity of the ZDDP tribofilm to the electron beam.

**Fig. 11** TEM images of NP tribofilm formed on steel surface, showing the **a** cross section of tribofilm, **b** chemical mapping of tribofilm, **c** EDS measurement from an area indicated as EDS spot in **a**, and **d, e** magnified view of areas 1 and 2 shown in **a**. Inner image in **c, d** shows the MoS<sub>2</sub> sheets



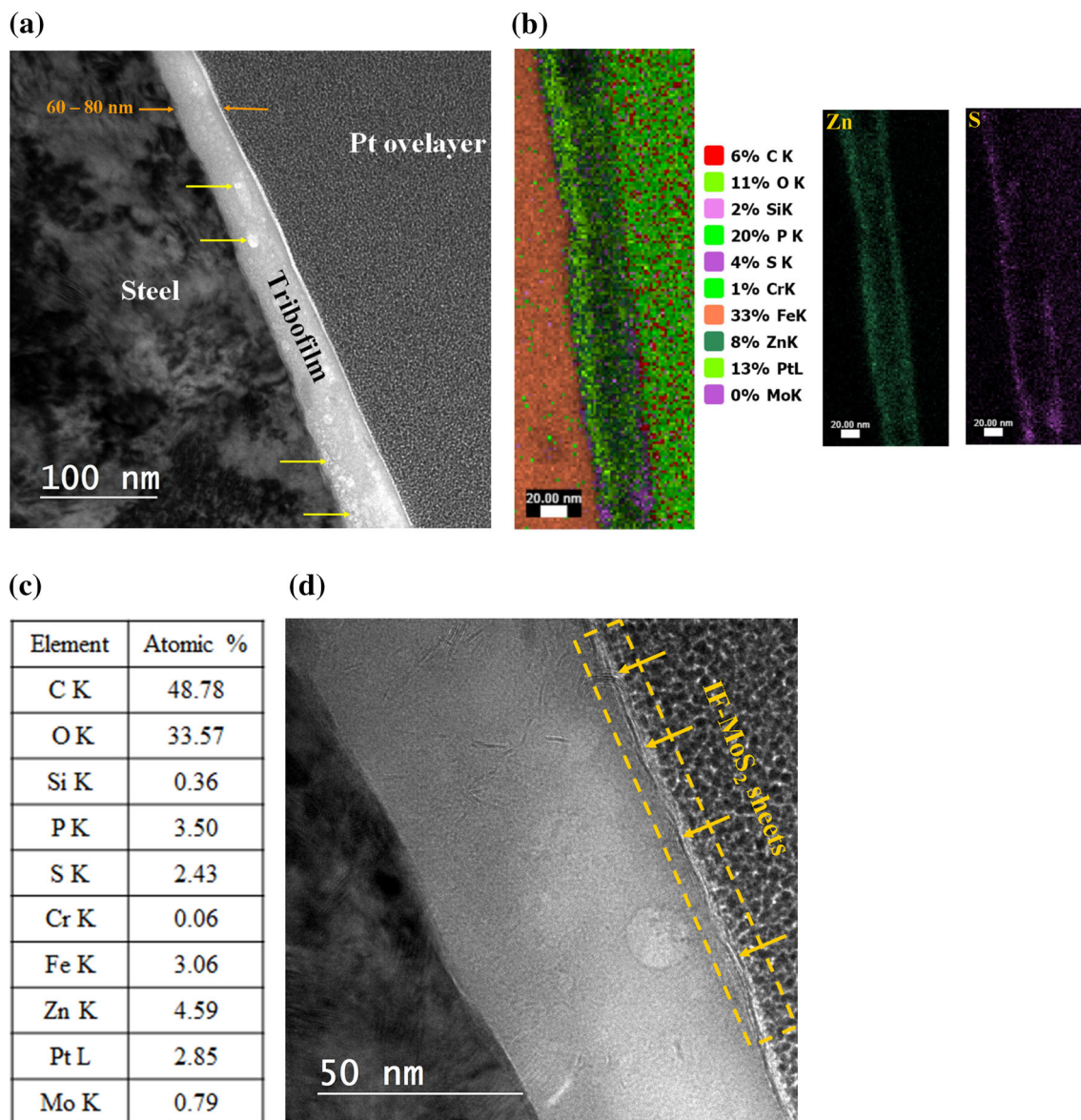


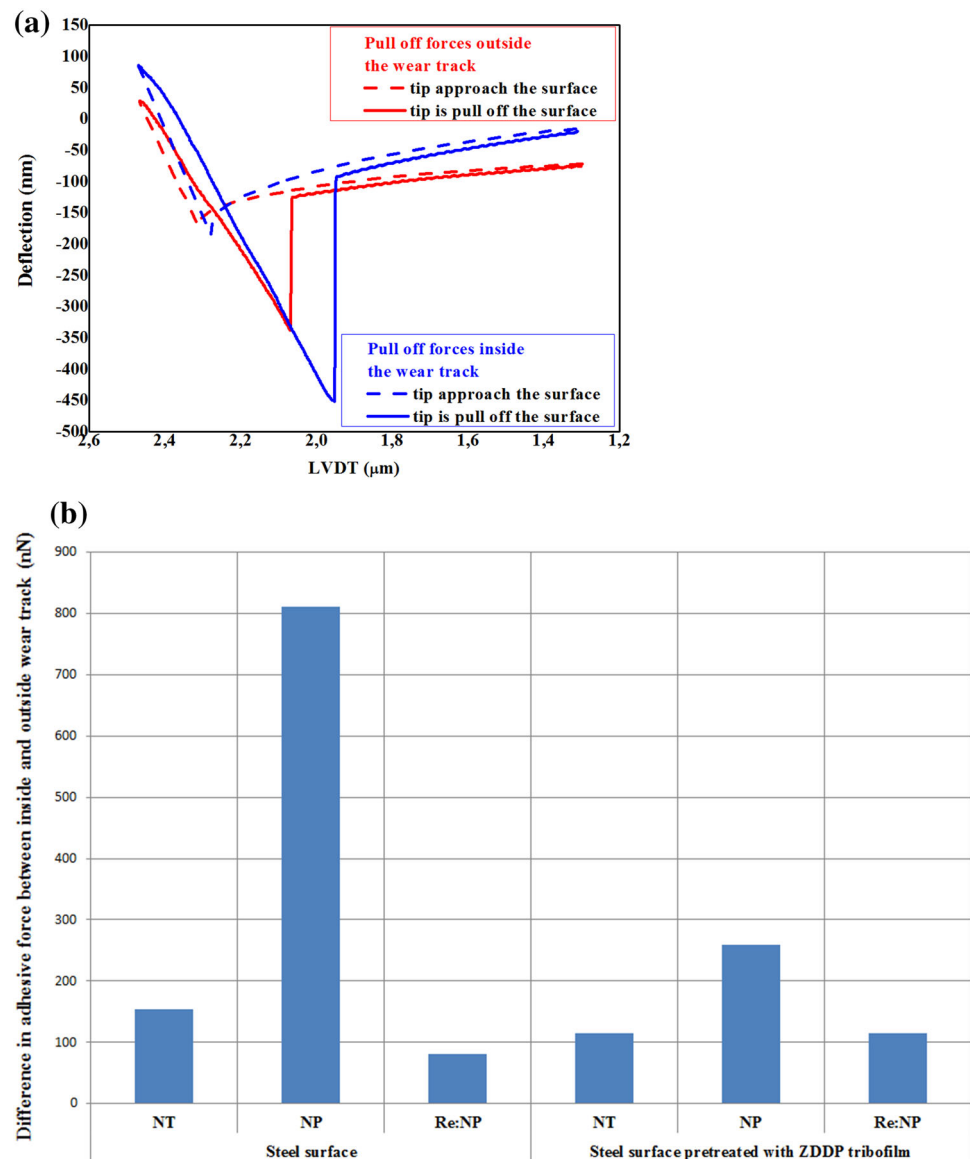
**Fig. 12** TEM images of NP tribofilm formed on ZDDP tribofilm-containing steel surface, showing the **a** cross section of tribofilm, **b** chemical mapping of tribofilm, **c** EDS measurement from mapped tribofilm, **d** exfoliated MoS<sub>2</sub> nanosheets on top of ZDDP tribofilm

Further TEM and EDX characterisation gave the evidence of a homogenous 60-nm-thick tribofilm composed of zinc phosphate compound (Fig. 12b, c), and MoS<sub>2</sub> sheets present mainly on the top of the tribofilm with thickness of 5–10 nm. Formation of MoS<sub>2</sub> nanosheets on the top of the tribolayer as a result of exfoliation is evident from Fig. 12d (indicated by arrows in the dashed rectangle and ellipse). Nevertheless, MoS<sub>2</sub>-derived products on the top layer did not degrade the structure of the ZDDP tribofilm as shown in the chemical mapping (Fig. 12b, c).

AFM force–displacement curves were generated as shown in Fig. 13a to test whether the nanoparticle-derived tribofilms show any difference in adhesion forces. When

the tip approached the surface, the tip snapped into contact from a few nanometres (5–7 nm) above the surface due to long-range interactive forces (5–10 nN). When the tip was retracted from the surface, the tip was deflected downward and kept in contact with the surface past the  $z = 0$  position until the cantilever deflection force was equal to the adhesive force, and then, it was suddenly pulled off the surface. This pull-off force was calculated using the tip deflection and spring constant, and one example of such a measurement is shown for MoS<sub>2</sub>-NT tested on steel surface in Fig. 13a. The difference in adhesive forces measured inside and outside the wear track for all nanoparticles investigated in this study is shown in Fig. 13b.

**Fig. 13 a** Force curves taken outside and inside the wear track for NP tested on steel surface (series I test) and **b** adhesive forces from outside and inside wear track for three nanoparticles investigated on steel and steel with preformed ZDDP tribofilm surfaces



## 4 Discussion

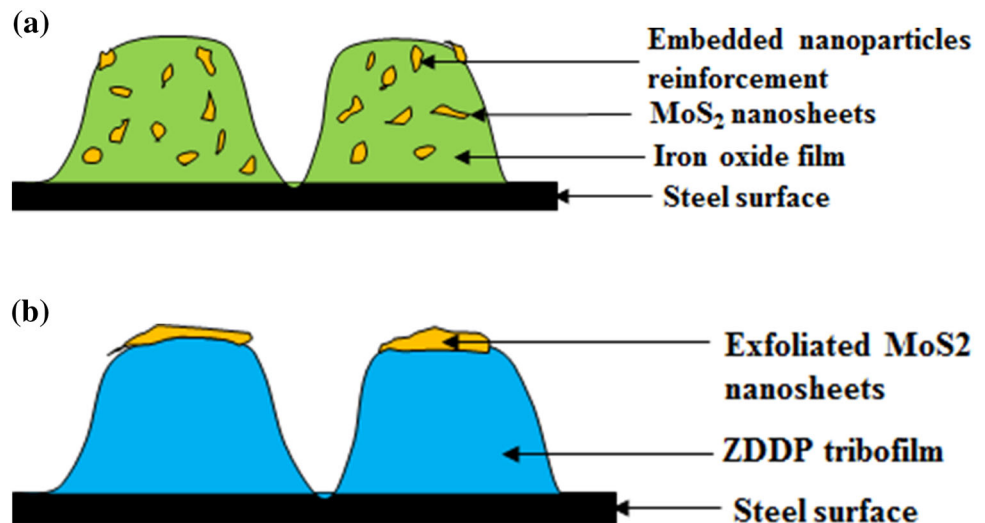
The results reveal interesting differences in terms of friction, wear and tribofilm formation between the three nanoparticles investigated in this study, and these parameters appear to depend on substrate type, for instance, steel or steel pretreated with ZDDP tribofilm. Some key features/differences are discussed below.

### 4.1 Lubricating Mechanism

Besides the difference in pad size structure, one might notice from Table 3 and Fig. 9b that NP-derived elements (i.e. Mo and S) were not observed in the tribofilm formed on steel surface pretreated with ZDDP additive. One explanation could be the low surface sensitivity to Mo and

S for the 20 keV electron beam (too deep penetration). Using low-energy electron beam (e.g. in the range 5–8 keV) may probably show higher concentration of NPs elements, but this was not verified. Although NP when tested on pretreated ZDDP surface (series II tests) showed significantly lower friction and slightly lower disc wear than when tested on steel surface (see Fig. 5), the absence of  $\text{MoS}_2$  in tribofilm (see EDX data shown in Fig. 9b) questions the responsible lubricating mechanism with these nanoparticles. Nevertheless, this can be explained by results obtained using TEM. The TEM cross section and analysis of the tribofilm formed from NP on bare steel surface (Fig. 11) have shown that thin IF- $\text{MoS}_2$  lamellar structures (10–15 nm: Fig. 11d) are embedded in the tribofilm (40–60 nm) in case of series I test. On the pretreated ZDDP surface in tests series II, exfoliated  $\text{MoS}_2$  nanosheets

**Fig. 14** Schematic diagrams showing the nature of nanoparticle-derived hybrid tribolayer formed on **a** steel surface (that formed iron oxide during test) and **b** preformed ZDDP-containing steel surface



(5–10 nm; Fig. 12d) are found on the top of tribofilm. These results suggest that in order to obtain significant benefits in terms of friction, it is important for particles to remain at the contact interface and that the friction benefit may be compromised when the particles get entrapped or exfoliated within the tribofilm.

In summary, formation of nanosheets was observed within the tribofilm formed on bare steel surface (iron oxide), and on the top layer of ZDDP tribofilm formed on steel surface with preformed ZDDP film. This appears to be one of the major differences in tribofilm formation mechanism, which depends on the base substrate material (iron oxide or ZDDP film). Additionally, the nanoparticles most probably get oxidised in the contact (in particular Re/IF-MoS<sub>2</sub> which are chemically less stable), so that the wear process is affected by both mechanisms.

#### 4.2 Influence of Nanoparticle-Derived Tribofilms on Adhesion

It can be seen from Fig. 13b that films formed from all nanoparticles on steel surface exhibited higher adhesive force compared to outside the wear track. This suggests the presence of some relatively soft films (formed from MoS<sub>2</sub>-NT, IF-MoS<sub>2</sub> and IF-Re:MoS<sub>2</sub>) inside the wear tracks, causing the AFM tip to stick strongly on to the surface, requiring larger forces to retract. Alternatively, considering the fact that films formed from these nanoparticles were not homogenous and that tip radius size is in nanometre scale (10 nm), it is hard to exactly locate nanoparticle-derived tribofilm while generating force curves. Thus, it could be possible that these measurements were made on bulk layer of tribofilm, which, as shown earlier, are predominantly either oxides (in case of series I tests) or ZDDP film (in

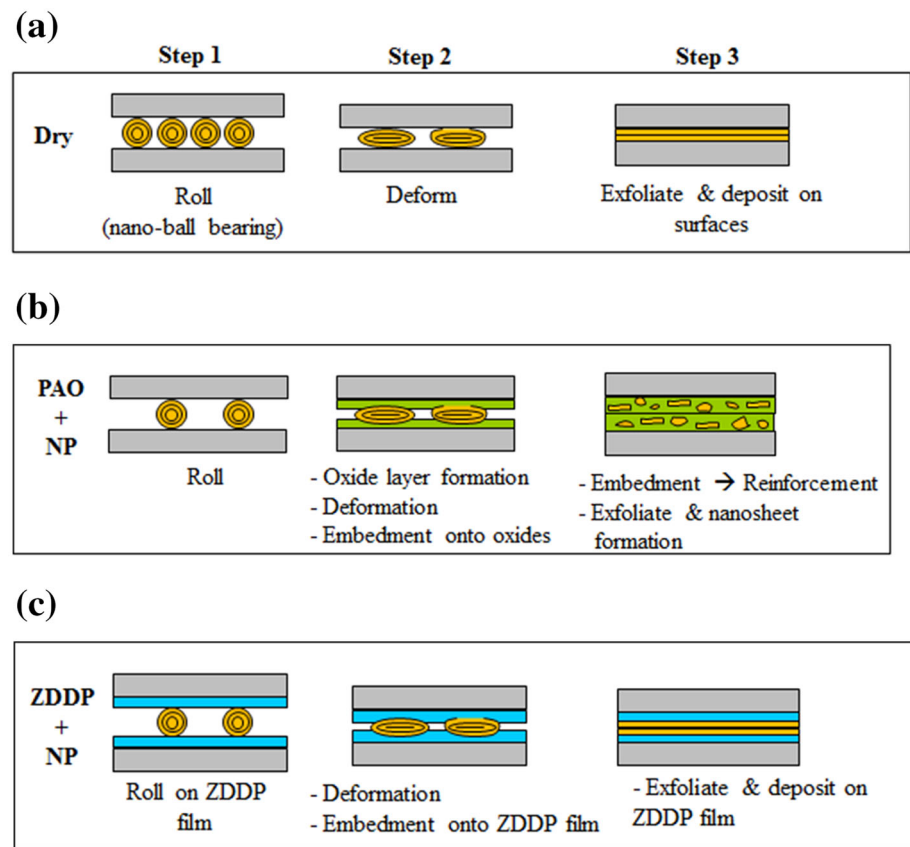
case of series II tests). So, it is obvious to see very high adhesive forces in nanoasperity interactions. However, such large adhesive forces are not reflected in friction measurements shown in Figs. 3 and 4 as these involve microasperity interactions.

#### 4.3 Influence of Substrate Type (Steel or Steel with ZDDP Tribofilm) on Friction and Wear

With steel surfaces, Re-doped nanoparticles were able to reduce friction by 70 % and MoS<sub>2</sub> nanoparticles by 30–40 % when compared to base oil. However, the friction evolution with nanotubes was unstable, and reproducibility of tests with nanotubes is questionable. This is due to different amounts of particles entraining into contact in each test. Also, there is no definite way of controlling these particles in order to make them stay in contact. This, in general, also depends largely on many factors including contact geometry, contact pressure and surface roughness. In order to reduce the influences from these parameters, steel surface with preformed ZDDP tribofilm was used to understand solely the effective tribological benefits of these nanoparticles. The results of IF-MoS<sub>2</sub> on steel surfaces with pretreated ZDDP tribofilm clearly indicate that nanoparticles were able to remain in contact, thus showing much stable and reduced friction soon after the test lubricant was changed from ZDDP to nanoparticles in series II tests. Also, the reduction in wear was significant for all three nanoparticles investigated in this study, four times lower wear in comparison with base oil and two times lower compared to ZDDP-additivated base oil.

In summary, IF-MoS<sub>2</sub> lamellar structures embedded in the iron oxide film were found for tests series I (Fig. 14a). The (iron) oxide layer formed on plain steel surface

**Fig. 15** Schematic diagram showing the lubrication process of MoS<sub>2</sub>-based nanoparticles/nanotubes **a** under dry condition, **b** in base oil (PAO) and **c** ZDDP-additivated PAO



provides a cushion base for nanoparticles, which allows embedment of the nanoparticles within the iron oxide surface, as shown schematically in Fig. 14a.

In test series II (prerubbing with ZDDP), exfoliated nanoparticles were found only on the top of the tribofilm surface (Fig. 14b). The preformed ZDDP tribofilm on the steel surface serves also as a cushion base and helps retaining nanoparticles in the contact. In addition, the nanoparticles get exfoliated and generate a hybrid layer on the top of the ZDDP tribofilm (probably top 10–20 nm of MoS<sub>2</sub> nanosheets) as shown schematically in Fig. 14b. Such exfoliated nanoparticles onto the ZDDP film acts as a good reinforcement and load-carrying membrane, thus exhibiting enhanced wear resistance properties. As wear results show, the hybrid layer formed on ZDDP tribofilm appears to be more wear resistant compared to that formed on iron oxide. This, further, assures that such nanoparticles are greatly compatible with the conventional anti-wear additive ZDDP without compromising the original AW properties of ZDDP films.

Besides all these, in general, whether the base is iron oxide or ZDDP tribofilm, the lubricating action appears to be similar (schematically presented in Fig. 15). This in order is (a) firstly nanoparticles just roll in the contact

acting more like a nanoball bearing (thus immediate friction reduction can be observed), followed by (b) embedment of nanoparticles on to the soft base matrix and possibly also entrapment into the matrix and finally (c) nanoparticles get exfoliated (as confirmed by TEM investigations) due to shear, allowing transfer of molecular sheets on to surface asperities. The exfoliation of nanoparticles (c) can also occur prior or simultaneously with embedment (b). The last step (exfoliation and transfer of molecular sheets) in this proposed mechanism was found to a great extent only with surfaces containing ZDDP film. This means the contact takes place on MoS<sub>2</sub> nanosheet-on-nanosheet, i.e. shear is between MoS<sub>2</sub> lamellar structure sheets, resulting in very low friction. These observations are in agreement with those proposed in [5, 9]. Furthermore, studies with MoS<sub>2</sub> nanoparticles and ZDDP anti-wear additive clearly highlight the synergism between them [9]. Preformed film of ZDDP appears to protect MoS<sub>2</sub> sheets from oxidation, thus leading to improved reproducibility and friction-reducing properties. At the same time, the presence of the ZDDP enhances the anti-wear properties of the MoS<sub>2</sub> nanoparticles, and also, the combination of ZDDP and nanoparticles show higher wear resistance than that typically seen solely with ZDDP alone.

#### 4.4 Durability of ZDDP Tribofilm After Running-in Nanoparticle Solution

Whether or not nanoparticles remove the preformed ZDDP tribofilms is interesting to know as this would further advance the potential use of MoS<sub>2</sub> nanoparticles/nanotubes as boundary lubricating additive for fully formulated lubricants. The series II tests was basically designed to evaluate this particular property of nanoparticles. It is evident from the cross section and chemical mapping of the tribofilm shown, respectively, in Fig. 11a, c that the ZDDP tribofilm remains intact without any degradation to its structure. A similar observation was made with all three nanoparticles. These results indicate that nanoparticles do not cause any damage to the preformed ZDDP tribofilm, so it is likely to expect a wear resistance at least similar to ZDDP and in addition, a significant reduction in friction. The wear results shown in Fig. 5 demonstrate this (disc wear in 10<sup>-18</sup> m<sup>3</sup>/nm with ZDDP = 0.8; NT = 0.7; NP = 0.4 and Re-NP = 0.6). Both ZDDP film and nanoparticles appear to be mutually helping each other. While nanoparticles do not degrade the structure of ZDDP film, ZDDP serves as a matrix for nanoparticles, allowing formation of nanosheets on top of ZDDP film. This means, ZDDP film provides the primary anti-wear role, and the MoS<sub>2</sub> nanosheets on top of ZDDP film acts as a friction modifier (FM), making this combination to serve a dual role (AW and FM). This highlights the perfect synergism between the nanoparticles investigated and ZDDP.

In summary, it can be concluded based on the results presented in this study that the lubrication process with nanoparticles can be categorised depending on the lubrication and contact conditions. This, for instance, is schematically illustrated in Fig. 15. When used under dry condition, nanoparticles follow the three most widely reported mechanisms, i.e. rolling, deforming and exfoliating, as shown in Fig. 15a. When used with oils (base oil or additivated oil), nanoparticles are likely to struggle entraining into contact as mobility of oil makes particles either settle down or move away from the contact, meaning that movement of nanoparticles are controlled by the bulk oil. For high-speed applications, this could be severe. It is believed that until the time nanoparticles manage to entrain into the contact, the contact surfaces are likely to get oxidised in case of base oil (Fig. 15b) and form ZDDP film in case of oil with ZDDP (Fig. 15c). This layer (oxide or ZDDP film) in turn helps acquiring nanoparticles as they act as matrix where nanoparticles could embed on to. Depending on the nature and hardness of the tribofilms formed, embedment could be mild (ZDDP film) or deeper (oxide). As the wear results demonstrate, significant exfoliation of nanoparticles on the top surface, as seen with

ZDDP film, means stronger reinforcement and enhanced strength of tribofilm and thus improved wear resistance.

## 5 Conclusions

1. MoS<sub>2</sub>-NT, nanoparticles and Re-doped nanoparticles reduced coefficient of friction by more than 50 % compared to base oil PAO4 in rubbing steel–steel tribo-pair contact.
2. Evidence of tribological interactions between MoS<sub>2</sub> nanosheets resulting from embedment of the IF-MoS<sub>2</sub> nanoparticles into oxide layer was shown.
3. In case of prerubbing tests with ZDDP, immediate strong reduction in CoF and wear rate after adding nanoparticles was noted, originate from exfoliation of nanoparticles on the top of the tribofilm surface.
4. In both test series, a 50- to 60-nm-thick tribofilm protecting the steel surface with exfoliated MoS<sub>2</sub> sheets was discovered.
5. Prerubbing with ZDDP benefit with high reproducibility of results and stable friction curve.

**Acknowledgments** The present work was carried out at the “Excellence Centre of Tribology”, Wiener Neustadt, Austria in the frame of Austrian COMET Programme (Project K2, Xtribology, No. 824187/849109). The authors kindly acknowledge Prof. Reshef Tenne for providing the IF-MoS<sub>2</sub> and Re/IF-MoS<sub>2</sub> nanoparticles used within the present work.

## References

1. Chhowalla, M., Amaratunga, G.A.J.: Thin films of fullerene-like MoS<sub>2</sub> nanoparticles with ultra-low friction and wear. *Nature* **407**, 164–167 (2000)
2. Hou, X.H., Shan, C.X., Choy, K.L.: Microstructures and tribological properties of PEEK-based nanocomposite coatings incorporating inorganic fullerene-like nanoparticles. *Surf. Coat. Technol.* **202**, 2287–2291 (2008)
3. Rapoport, L., Fleischer, N., Tenne, R.: Applications of WS<sub>2</sub> (MoS<sub>2</sub>) inorganic nanotubes and fullerene-like nanoparticles for solid lubrication and for structural nanocomposites. *J. Mater. Chem.* **15**, 1782–1788 (2005)
4. Reddy, N.S.K., Nouari, M., Yang, M.: Development of electrostatic solid lubrication system for improvement in machining process performance. *Int. J. Mach. Tools Manuf.* **50**, 789–797 (2010)
5. Wiesel, I., Arbel, H., Albu-Yaron, A., Popovitz-Biro, R., Gordon, J.M., Feuermann, D., Tenne, R.: Synthesis of WS<sub>2</sub> and MoS<sub>2</sub> fullerene-like nanoparticles from solid precursors. *Nano Research* **2**(5), 416–424 (2009)
6. André, B., Gustavsson, F., Svahn, F., Jacobson, S.: Performance and tribofilm formation of a low-friction coating incorporating inorganic fullerene like nano-particles. *Surf. Coat. Technol.* **206**(8–9), 2325–2329 (2012)
7. Jenei, I.Z.: Scanning electron microscopy (SEM) analysis of tribofilms enhanced by fullerene-like nanoparticles. Licentiate thesis, Stockholm University, Sweden (2012)

8. Rosentsveig, R., Margolin, A., Gorodnev, A., Popovitz-Biro, R., Feldman, Y., Rapoport, L., Novema, Y., Naveh, G., Tenne, R.: Synthesis of fullerene-like MoS<sub>2</sub> nanoparticles and their tribological behavior. *J. Mater. Chem.* **19**, 4368–4374 (2009)
9. Yadgarov, L., Stroppa, D.G., Rosentsveig, R., Ron, R., Enyashin, A.N., Houben, L., Tenne, R.: Investigation of rhenium doped MoS<sub>2</sub> nanoparticles with fullerene-like structure. *Zeitschrift für Anorganische und Allgemeine Chemie: ZAAC* **638**, 2610–2616 (2012)
10. Tannous, J., Dassenoy, F., Lahouij, I., Le Mogne, T., Vacher, B., Bruhacs, A., Tremel, W.: Understanding the tribochemical mechanisms of IF-MoS<sub>2</sub> nanoparticles under boundary lubrication. *Tribol. Lett.* **41**, 55–64 (2011)
11. Kalin, M., Kogovšek, J., Remškar, M.: Nanoparticles as novel lubricating additives in a green, physically based lubrication technology for DLC coatings. *Wear* **303**, 480–485 (2013)
12. Yadgarov, L., Petrone, V., Rosentsveig, R., Feldman, Y., Tenne, R., Senatore, A.: Tribological studies of rhenium doped fullerene-like MoS<sub>2</sub> nanoparticles in boundary, mixed and elasto-hydrodynamic lubrication conditions. *Wear* **297**, 1103–1110 (2013)
13. Rabaso, P., Ville, F., Dassenoy, F., Diaby, M., Afanasiev, P., Cavoret, J., Vacher, B., Le Mogne, T.: Boundary lubrication: Influence of the size and structure of inorganic fullerene-like MoS<sub>2</sub> nanoparticles on friction and wear reduction. *Wear* **320**, 161–178 (2014)
14. Kogovsek, J., Remskar, M., Mrzel, A., Kalin, M.: Influence of surface roughness and running-in on the lubrication of steel surfaces with oil containing MoS<sub>2</sub> nanotubes in all lubrication regimes. *Tribol. Int.* **61**, 40–47 (2013)
15. Rabaso, P., Dassenoy, F., Ville, F., Diaby, M., Vacher, B., Le Mogne, T., Belin, M., Cavoret, J.: An investigation on the reduced ability of IF-MoS<sub>2</sub> nanoparticles to reduce friction and wear in the presence of dispersants. *Tribol. Lett.* **55**(3), 503–516 (2014)
16. Aldana, P.U., Vacher, B., Mogne, T., Belin, M., Thiebaut, B., Dassenoy, F.: Action mechanism of WS<sub>2</sub> nanoparticles with ZDDP additive in boundary lubrication regime. *Tribol. Lett.* **56**(2), 249–258 (2014)
17. Naveira Suarez, A., Tomala, A., Pasaribu, R., Larsson, R., Gebeshuber, I.C.: Evolution of ZDDP-derived reaction layer morphology with rubbing time. *Scanning* **32**(5), 294–303 (2010)
18. Vengudusamy, B., Green, J.H., Lamb, G.D., Spikes, H.A.: Tribological properties of tribofilms formed from ZDDP in DLC/DLC and DLC/steel contacts. *Tribol. Int.* **44**, 165–174 (2011)
19. Spikes, H.A.: The history and mechanisms of ZDDP. *Tribol. Lett.* **17**, 469–489 (2004)
20. Vengudusamy, B., Green, J.H., Lamb, G.D., Spikes, H.A.: Influence of hydrogen and tungsten concentration on the tribological properties of DLC/DLC contacts with ZDDP. *Wear* **298–299**, 109–119 (2013)